Journal of Engineering Science and Technology
Vol. 14, No. 4 (2019) 1878 - 1892

EBG LOADED COMPACT WIDE-NOTCH BAND ANTENNA WITH FREQUENCY RECONFIGURABLE CHARACTERISTICS

M. L. S. N. S. LAKSHMI, B. T. P. MADHAV*,
HABIBULLA KHAN, P. PARDHASARADHI

Antenna and Liquid Cystals Research Centre, Research and Development (ALRC-R&D)
Department of Eletronics and Computer Engineering (ECE), Koneru Lakshmaiah,
Education Foundation, Vaddeswaram, AP, India
*Corresponding Author: btpmadhav@kluniversity.in

Abstract

A novel circular slot antenna with EBG loading is presented in this work to attain wide notch band characteristics. Quad notch bands are attained at 1.8-3.1 GHz (PCS, UMTS, Bluetooth, LTE, etc.), 3.3-5.3 GHz (Wi-Fi, etc.), 5.5-8.7 GHz (WLAN, etc.) and 9.8-10.8 GHz (Satellite Communication applications etc.,) respectively. To extend the notch bandwidth, a planar electromagnetic bandgap structure is introduced in the ground plane. The designed antenna is occupying the compact dimension of 44×40×1.6 mm on FR4 substrate with dielectric constant 4.4 and loss tangent 0.02. The simulation and the optimization are done with CST microwave studio tool and the prototyped antenna on Nvis 71 related measurements are analysed in anechoic chamber with the help of combinational analyzer and antenna measurement setup.

Keywords: Compact antenna, Electromagnetic bandgap (EBG), Notch band, Reconfigurability.

1. Introduction

The frequency diversity is the most useful thing for communication systems, where the reuse of multiple operations is needed. This will give rise to the antennas with frequency reconfigurability, polarization reconfigurability and pattern reconfigurability. The antenna with any of the reconfigurable nature or hybrid reconfigurability got tremendous attention these days to use smartly in most of the communication systems. Prior to this, the additional characteristics such as low cost, compact dimension and multipurpose functions with integration to wireless systems attracting the antenna designers to design advanced reconfigurable antennas.

A novel ultracompact reconfigurable antenna was proposed by Javier Leonardo [1] for wideband frequency reconfigurability. The optimization process of the antenna and the switching patterns are carried out by genetic algorithm. Tamer aboufoul presented a reconfigurable and notched tapered slot ultra wideband antenna for cognitive radio applications in [2]. Tapered slot is electrically coupled to resonator parasitic microstrip line to notch the specific frequency band and by changing the length of the stub, the impedance matching is varied for frequency tunability. Ren et al. [3] designed a frequency tuneable antenna with unequal U-slot structure, which is providing average gain more than 4.5 dB. The designed antenna with lumped variable varactors managed to tune the antenna at six different frequencies between 2.3 to 3.6 GHz and the size is 30% less when compared with conventional U-slot antenna. Qiu et al. [4] proposed a novel pattern and frequency reconfigurable antenna with parasitic array. The driven patch with RF-PIN diodes connection invoking the antenna's tunability at 2.1, 2.4 and 2.6 respectively.

Cheng et al. [5] designed a compact microstrip antenna for polarization diversity with reconfigurable feed. Four triangular shaped elements are used as radiating patch to obtain linear polarization, left-hand circular polarization and right-hand circular polarization. Wilkinson power divider with PIN diodes connections are used to interlink the four patch elements. Li et al. [6] proposed a polarization reconfigurable metamaterial inspired antenna with complementary split ring resonators. PIN diodes are mounted on the ground plane slot to attain the polarization reconfigurability in the antenna. Planar EBG structure is also introduced to extend the bandwidth of axial ratio.

Rajeshkumar and Raghavan [7] proposed a metamaterial inspired triple band reconfigurable antenna for WLAN/WiMAX applications. The triple band antenna providing the impedance bandwidth of 18.6%, 4.3% and 40.3% at 2.4, 3.5 and 5 GHz bands respectively. Aghdam and Bagby [8] designed a reconfigurable filtering band in ultra wideband antenna. The designed antenna supporting the bands between 2 to 6 GHz and avoiding UWB interference with narrowband functionality. Horestani et al. [9] proposed reconfigurable S-shaped resonators in band notched ultra wideband antennas. In this model, S-SRR coupled to coplanar wave guide to provide the stop band in the transmission characteristics of the line. Qin et al., [10] proposed polarization reconfigurable antenna for wireless local area network applications. The PIN diodes will alter the length of the U-slot and intern the polarization will be affected. Circular polarization is achieved from 5.725 GHz to 5.8 GHz with axial ratio bandwidth more than 2.8%.

Sun et al. [11] proposed a compact triple band switchable antenna is designed for navigation systems. The reconfigurable nature is attained via a circular rotational manual motion. Li et al. [12] proposed frequency reconfigurable bow-tie

antenna for Bluetooth, WiMAX and WLAN applications. A simple biasing circuit is used to eliminate the extra biasing lines. Panahi et al. [13] proposed a simple polarization reconfigurable monopole antenna for wireless applications. Ground connection is provided through conductive strips to attain additional modes in circular polarization. Yu et al. [14] proposed a planar loop monopole reconfigurable antenna for mobile handsets. The designed antenna operating in the GSM, LTE2300, WLAN, LTE2500, DCS, PCS and UMTS bands with coverage of 2G/3G/4G. Madhav et al. [15] proposed a frequency reconfigurable monopole antenna with defected ground structure for ISM band applications. BAR64-02V PIN diodes are used for the switching of the antenna between 2.2 to 2.5 GHz with peak realized gain of 3.2 dB.

A compact frequency reconfigurable antenna with EBG loading for wide-notch band switching is presented in this work. The main motivation in the design of the antenna is to attain the reconfigurable property and it can reject some frequency bands to attain the notch band characteristics. The antenna also provides multi band characteristics with considerable gain characteristics. The antenna is compact structure with considerable gain and efficiency. The antenna design considerations and the analysis of the obtained results are presented in the subsequent sections.

2. Antenna Geometry

The EBG loaded reconfigurable antenna is constructed with the modification in the circular monopole with slots for notching. Su [16] proposed the circular monopole, in which, is constructed based on the mathematical formulation and the actual radius of the circular patch was calculated. Slots are introduced in the radiating structure to attain the notching characteristics in the wide operating band. FR4 substrate of permittivity 4.4 and loss tangent 0.02 is used in the antenna design.

$$R = \frac{F}{\frac{2h}{1+\sqrt{\pi\varepsilon_{eff}F\left[\ln\frac{F\pi}{2h}+1.7726\right]}}} \tag{1}$$

$$F = \frac{8.791*10^{9}}{f_r\sqrt{\varepsilon_{eff}}} \tag{2}$$

where f_r = Resonant Frequency in Hz, ε_{eff} = Effective dielectric constant, R = Radius of the patch, h = Height of the substrate in mm. Slots are loaded on the radiating element to filter certain bands, which avoids the interference between UWB and other wireless services. To obtain the desired bands rejection, the slot dimensions are optimized with following equations.

$$\left(S_4 + S_2 + S_7 - 2P_1\right) = L_1 = C/4f_{notch}\sqrt{\varepsilon_{eff}} \tag{3}$$

where L_1 is the length of the upper slot, c is the velocity of light and f_{Notch} is the notch frequency.

$$\varepsilon_{eff} = (\varepsilon_r + 1)/2 \tag{4}$$

The lower slot dimensions are optimized from the following equations:

$$S_5 + 2S_6 - 2P_2 = L_2 = \lambda_{guided} / 2 \tag{5}$$

$$\lambda_{guided} = \frac{C}{f_{Notch}\sqrt{\varepsilon_{eff}}} \tag{6}$$

where λ_{guided} is the notch frequency guided wavelength and L_2 is the lower slot length.

The basic structure of the antenna is further modified by placing the U-shaped slot on the radiating patch with length of S_6 and width of S_5. In the antenna 3 is further modified with the extra rectangular slot for attaining the notch band characteristics. The same inverted rectangular slot is inserted exactly opposite with EBG structure in the ground plane to attain the proposed antenna structure.

Figure 1 shows the antenna iteration from basic circular monopole to double slot structure. Figure 2 shows the proposed antenna front and back view with dimensional characteristics in Table 1.

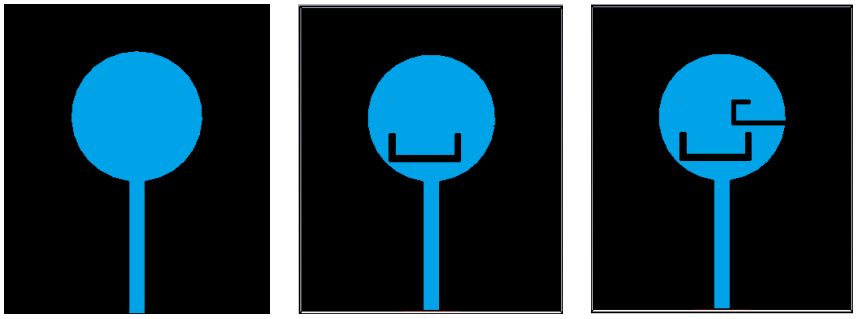

(a) (b) (c)

Fig. 1. Antenna iterations: (a) Antenna 1, Circular monopole, (b) Antenna 2: U-shaped slot monopole, (c) Antenna 3: Double slot monopole.

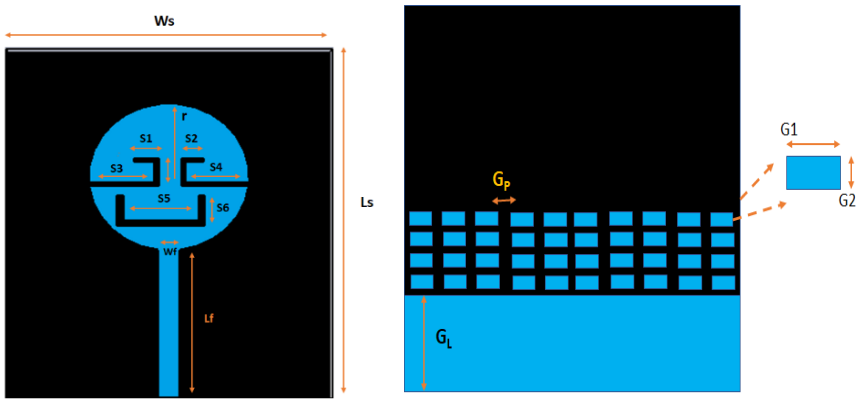

(a) (b)

Fig. 2. Proposed antenna: EBG loaded wide-notch antenna: (a) Front view, (b) Back view.

Table 1. Antenna dimensions (mm).

Parameter	Dimension	Parameter	Dimension	Parameter	Dimension
G_1	2.5	L_s	48	S_4	8.5
G_2	2	r	10	S_5	11
G_L	9.3	S_1	2.8	S_6	4.2
G_P	1.4	S_2	2.8	W_f	2.6
L_f	20	S_3	8.5	W_s	40

3. Results and Discussion

The proposed antenna is designed and analysed using commercial electromagnetic tool CST. The reflection coefficient of the antenna iterations is presented in Fig. 3. Antenna model 1 is working in the wideband from 2.6 to 11 GHz with bandwidth of 8.8 GHz.

The antenna model 2 is resonating at dual band of 1.8-2.2 GHz and 3.2 to 12 GHz with bandwidth of 400 MHz and 8.8 GHz respectively. Antenna 2 is providing notch band characteristics from 2.2 to 3.2 GHz with 1000 MHz notch bandwidth.

Antenna 3 is providing dual notch band characteristics at 2.2-3.3 GHz and 4.2-5.2 GHz respectively. The proposed antenna model with three slots in the radiating structure is providing quad notch bands from 1.8 to 2.6 GHz, 2.8 to 4.6 GHz, 4.8 to 7.2 GHz and 8 to 8.8 GHz. The u-shaped slots in the patch invoked the notch bands with notch bandwidths of 800 MHz, 1800 MHz, 2400 MHz and 800 MHz respectively.

The notch bandwidths are in the ratio of 1:2.4:3:1 with band stop characteristics for PCS, UMTS, Bluetooth, Wi-Fi, WLAN and mobile satellite applications and pass band characteristics for GPS, GSM, ISM, INSAT, Radio Altimeter and fixed satellite applications.

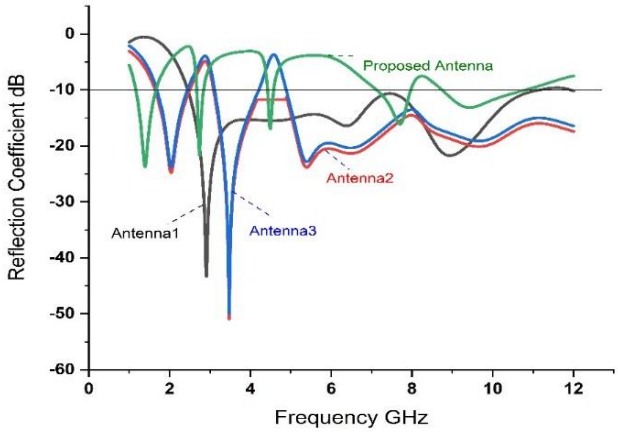

Fig. 3. Reflection coefficient of the antenna iterations.

If the antenna impedance is matched to the transmission line at resonance, the mismatch off resonance is related to the voltage standing wave ratio (VSWR). The reflection coefficient of < -10 dB and VSWR < 2 in the operating bands can be observed from Fig. 4. At fundamental notch band the rejection is very sharp (greater than -5 dB) and at other notch bands its level was slightly reduced in VSWR curve. A perfect matching between VSWR and the reflection coefficient with respect to the operating bands and the notch bands can be observed from Fig. 4.

The effect of some important dimensional parameters of the antenna are varied to optimize the model before fabrication. The dimensions are fixed after performing the parametric analysis and in this case, some significant parameters like Ground length G_L and feed width W_f are taken for parametric analysis. Other dimensional parameters are also analysed, but those are not affecting the performance characteristics of the antenna in a remarkable way. When length of the ground is varied from 9 to 9.5 mm, the optimized performance with respect to the targeted applications are found at 9.3 mm only and presented the same in Fig. 5. The width of the feed is also tuned from 2.4 to 2.8 mm with variation of 0.2 mm.

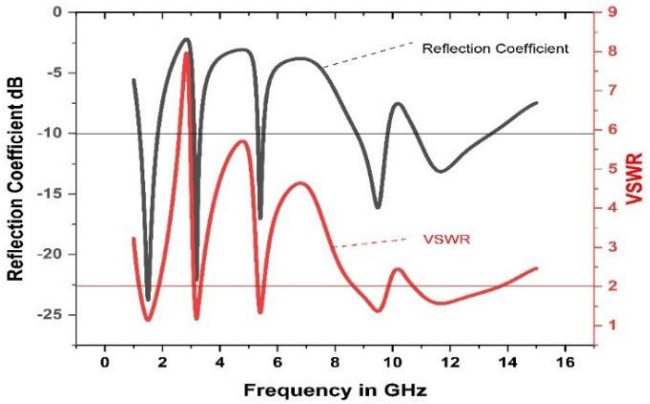

Fig. 4. Proposed antenna reflection coefficient and VSWR.

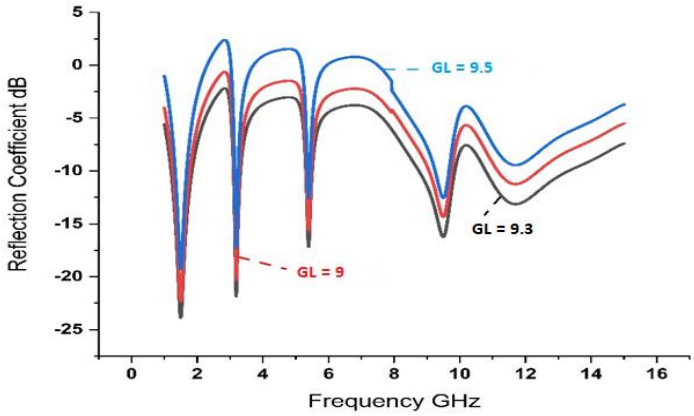

Fig. 5. Parametric analysis with change in ground length 'G_L'.

Based on Fig. 6, we found that 2.6 mm dimension is providing significant results with respect to the specific application-oriented bandwidth. The dimensions for ground length and feed width are optimized with parametric analysis in CST studio.

The surface current distribution characteristics of the proposed antenna at 1.56 GHz (GPS), 3.1 GHz and 5.8 GHz (WLAN) are presented in Fig. 7. The current intensity is focussed more at feed line and on the slots for lower operating band of 1.56 GHz. At 3.1 GHz, lower slot only participating in the radiation with high current density along with the feed line. At 5.8 GHz, the left most slot and lower slot are providing the radiation along with feed line, but the density is less when compared with lower band radiation characteristics.

Figure 8 shows the 3D gain plots for the proposed antenna at different operating bands. A peak realized gain of 3.4 dB at 2.4 GHz, 4 dB at 5.8 GHz and 3 dB at 10 GHz respectively. Figure 9 conveys the variation of gain with respect to different operating and notch bands.

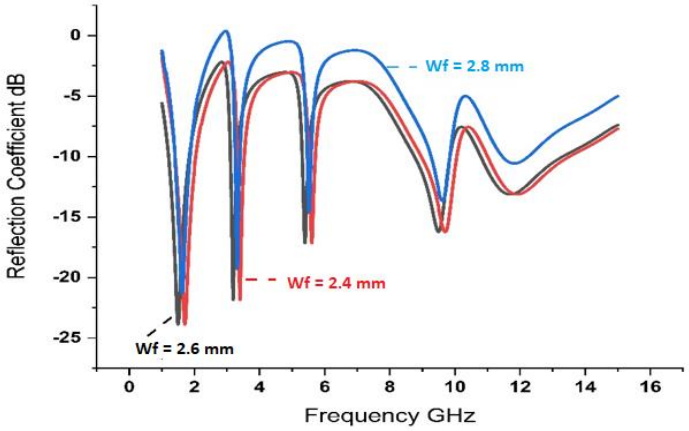

Fig. 6. Parametric analysis with change in width of the feed W_f.

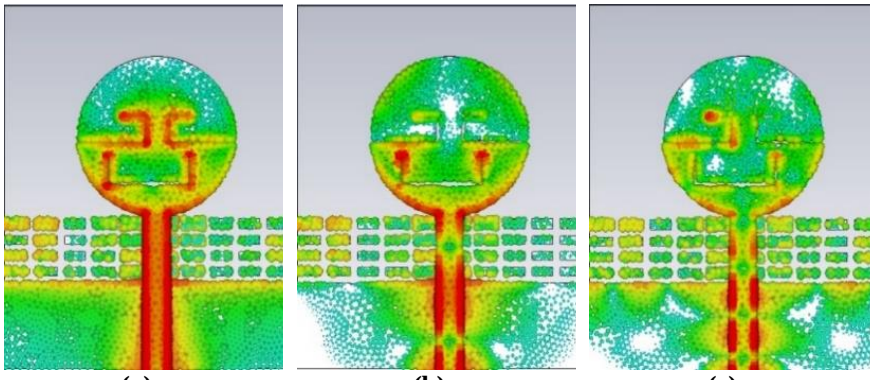

(a) **(b)** **(c)**

Fig. 7. Surface current distribution at 1.56 GHz, 3.1 GHz and 5.8 GHz.

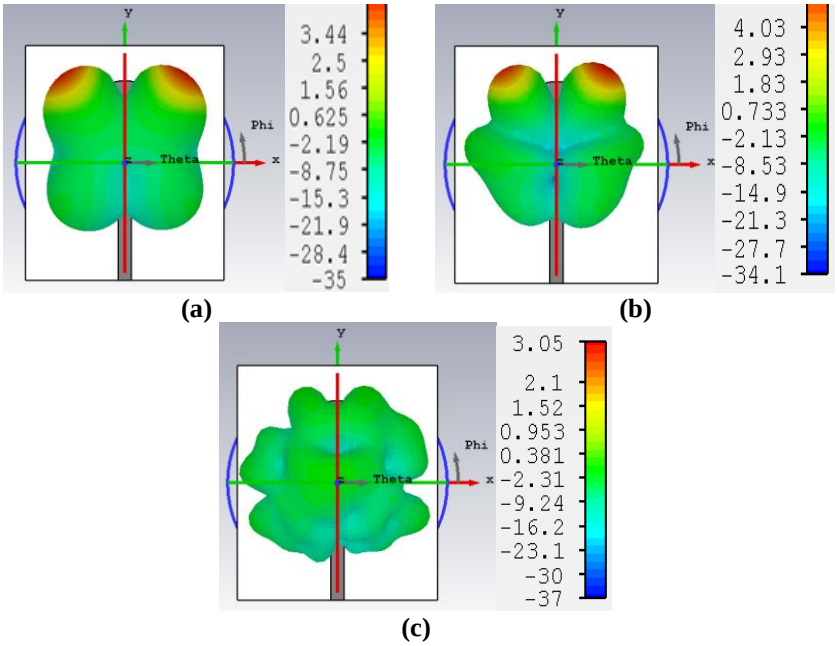

Fig. 8. 3D Radiation patterns: (a) 2.4 GHz, (b) 5.8 GHz, (c) 10 GHz.

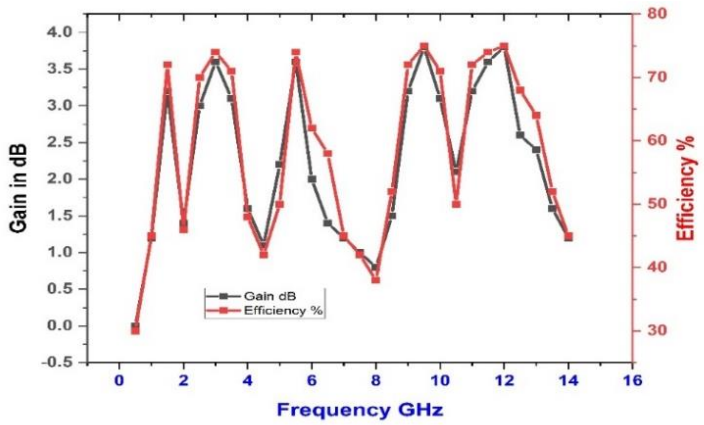

Fig. 9. Measured frequency vs. gain and efficiency.

The basic notch band antenna is fabricated on FR4 substrate and connected with 50 ohms SMA connector for measurement. Figure 10 shows the prototyped antenna front and back view and the measurement result of reflection coefficient with Anritsu combinational analyser.

A perfect matching of simulation and the measurement results can be observed from Fig. 11. At lower operating band almost 90 to 95% correlation is observed between measurement and simulation results. At higher operating band, little bit variation is observed due to connector mismatch and dielectric loss.

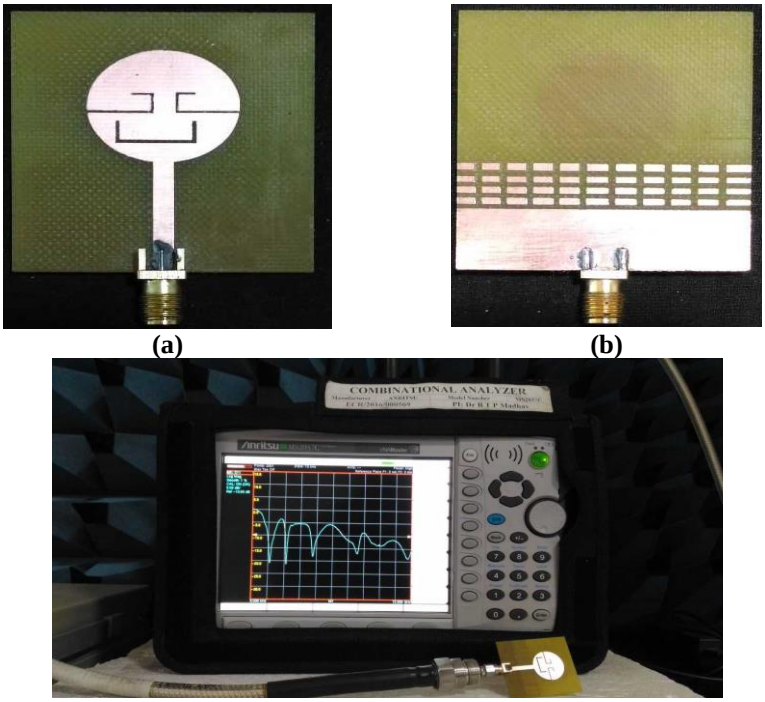

(a) **(b)**

(c)

Fig. 10. Fabricated notch band antenna: (a) Top view, (b) Bottom view, (c) Measurement on VNA.

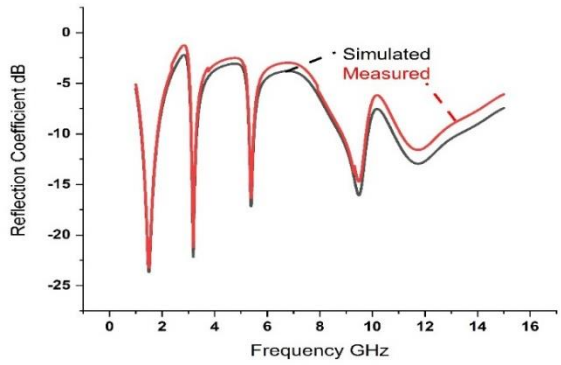

Fig. 11. Measured and simulated reflection coefficient.

4. Frequency Reconfigurability

The designed wide-notch band antenna is tested for its reconfigurable nature by placing BAR64-02V PIN diodes at slots on the radiating element as shown in the Fig. 12. The diode at middle slot is D1, diode at right side slot is D2 and the diode at left side slot is D3. The diodes are controlled by the bias voltage through RF chokes. The biasing voltage applied to RF choke, which is connected in series with the bias line and allows the DC current to flow through the patch finally biasing the diodes.

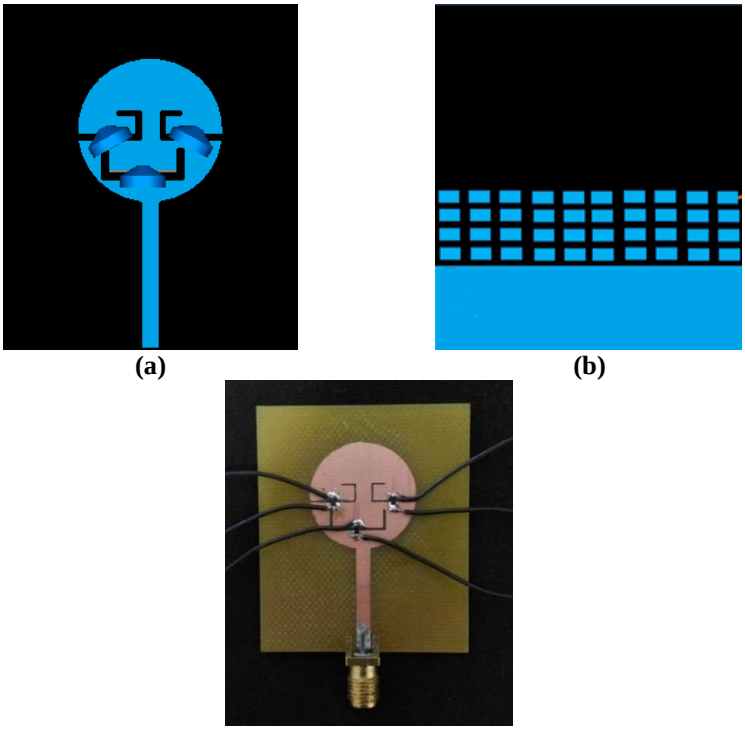

Fig. 12. Diodes placement on the proposed antenna: (a) Top view, (b) Bottom view, (c) Fabricated prototype.

After passing through each RF choke, the electric current completes its path. The anodes of PIN diodes are connected to lower side of the slots and the cathodes are connected on the upper side. The purpose of RF choke is to isolate DC bias circuit and RF circuit.

The three diodes can be switched on and off with eight combinations and at each combination the corresponding shift in the notch band and the operating band is recorded. The major frequency tunability cases with respect to the diode switching conditions are presented in Fig. 13 and tabulated the performance characteristics in Table 2.

The *S* parameters results are analysed when diodes are in OFF condition first and after that with different combinations and finally with all diodes in ON condition. The corresponding reconfigurable results are presented in Fig. 13.

The results are almost identical when diodes are in OFF condition, but small deflections are observed when diodes are turned ON. This deflection is due to the insertion loss by the diodes and the small imperfection in the connection of diodes between slots. The frequency reconfigurability is examined for diode switching conditions of D1D2D3 = 000 and D1D2D3 = 111 and presented the analysis in Fig. 14. There is a shift of almost 1.8 GHz between these two cases for fundamental resonant frequency and a good correlation between simulation and the measurement is observed for both the cases.

Table 2. Reconfigurable characteristics for diode switching conditions.

S. No.	D1	D2	D3	Operating band 1 (GHz)	Band 2	Band 3	Band 4	Band 5	Average gain (dB)	Average efficiency (%)
1	0	0	0	1-2 GHz	3-3.4 GHz	5.4-5.8 GHz	9-10 GHz	11-13 GHz	2.9 dB	65%
2	1	0	0	1.2-1.8 GHz	3.1-3.5 GHz	5.5-5.95 GHz	9.1-10.1 GHz	11.2-13.1 GHz	2.6 dB	64%
3	0	1	0	1.3-1.9 GHz	3.2-3.7 GHz	5.7-6.1 GHz	9.2-10.2 GHz	11.3-13.4 GHz	2.7 dB	64%
4	0	0	1	1.6-2.1 GHz	3.5-3.9 GHz	5.9-6.3 GHz	9.4-10.5 GHz	11.5-13.8 GHz	2.5 dB	62%
5	1	1	1	1.8-2.2 GHz	3.6-4.2 GHz	6-6.4 GHz	9.5-10.6 GHz	-	2.8 dB	64%

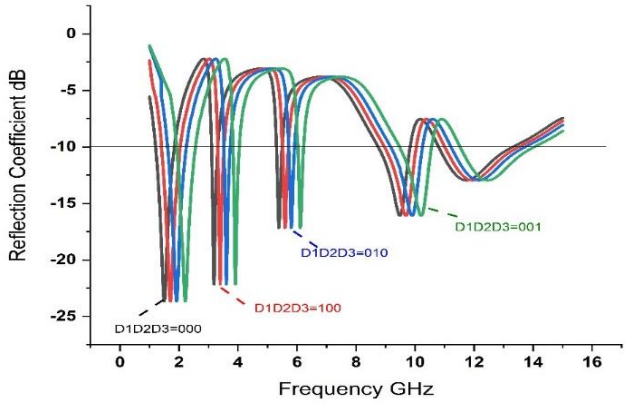

Fig. 13. Frequency reconfigurability with diode conditions (000, 100, 010, 001,111).

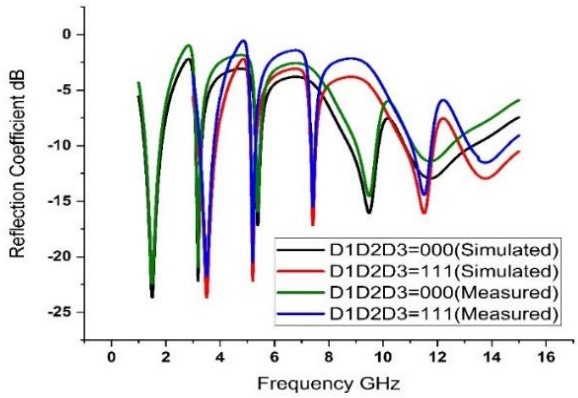

Fig. 14. Simulated and measured reflection coefficient for diode conditions.

The development in modern communication, satellite navigation and in other fields like remote sensing, the group delay measurements are playing important role. The group delay can be calculated with the given formula [17].

$$GD(f) = \frac{1}{360}\frac{d\phi(f)}{df} \tag{7}$$

where $GD(f)$ is the group delay in seconds, $\phi(f)$ is the phase function in the degrees and f is the frequency in GHz. At fixed distances, the measurement error caused by multiple reflections between transmitting and receiving antennas will

be considered. The group delay result for the proposed antenna model is presented in Fig. 15.

As the operating bands goes to higher frequencies, the perturbations caused by discontinuties will play a significant role. These perturbations can be reduced with time domain reflectometer techniques. The reflected signal provides the significant information regarding the testing instrument. Figure 16 provides the information regarding the distortion occurred at different time intervals when testing instrument is connected to the antenna.

From the reference Table 3 it is observed theat the antenna size is compact with the previous literature and also provides the notch band characteristics and operates with gain of above 3 dBi. However, the efficiency of the antenna is low with compared prevuious literatue available.

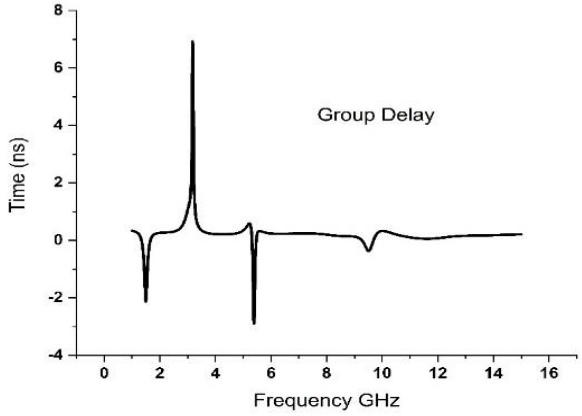

Fig. 15. Frequency vs. group delay.

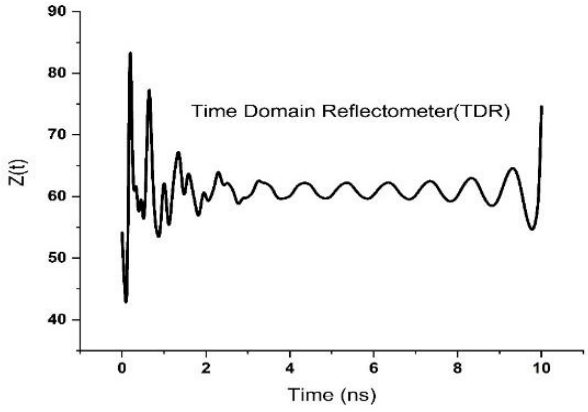

Fig. 16. Time vs. TDR.

Table 3. Comprassion of references.

Reference	Antenna size	No. of diodes	Frequency (GHz)	Gain (dBi)	Efficiency (%)
Quijano and Vecchi [1]	58×78×1.534	-	2.45-2.5	4.39	95.37
Aboufoul et al. [2]	27×16×1.52	2	3-4	2.1	90
			4.5-5.5	0.8	40
Horestani et al. [9]	49.4×35×0.2	2	3.2	8.5	45
Qin et al. [10]	40×40×1.6	2	5.6-6.3	6.3-7.5	82
Panahi et al. [13]	35.2×67.4×1.52	2	2.4	1.74	-
Su [16]	100×75×75	-	2.4-2.484	2.4	77
			5.15-5.825	3.1	79
Proposed model	48×40×1.6	3	1.4-1.8	3.5	71
			2.6-3	3.3	73
			4.3-4.5	3.6	73
			7.2-8.1	3.3	72

5. Conclusion

A frequency reconfigurable wide-notch band antenna is designed and analysed in this work. Electromagnetic bandgap loading is used in the antenna structure to improve the impedance bandwidth. Antenna is fed with microstrip line feeding of impedance 50 ohms and the wide-notch band characteristics are obtained through the slots placed on the circular radiating structure.

The designed antenna providing Quad notch bands at 1.8-3.1 GHz (PCS, UMTS, Bluetooth, LTE, etc.,), 3.3-5.3 GHz (Wi-Fi, etc.,), 5.5-8.7 GHz (WLAN, etc.,) and 9.8-10.8 GHz (Satellite Communication applications etc.,) respectively. The measured results are providing excellent correlation with the simulation results for the validation of the proposed antenna in the practical applications.

Acknowledgements

Authors like to thank KLEF ECE department for their moral support and DST for technical support through ECR/2016/000569, EEQ/2016/000604.

Nomenclatures

c	Velocity of light, m/s
f	Frequency, GHz
f_r	Resonant frequency, GHz
G_D	Group delay, ns
G_L	Ground length, mm
G_p	Gap in EBG, mm
h	Height of substrate, mm
L_f	Feed length, mm
L_s	Length of substrate, mm
R	Radius of patch, mm
S_1	Left upper slot length , mm
S_2	Right upper slot length, mm
S_3	Left lower slot length, mm
S_4	Right lower slot length, mm
S_5	Middle slot length, mm

W_f	Feed width, mm
W_s	Width of the substrate, mm

Greek Symbols

$\mathcal{E}_{eff}$	Effective dielectric constant
$\mathcal{E}_r$	Dielectric constant
$\Phi_{(f)}$	Phase function

Abbreviations

LTE	Long Term Evolution
PCS	Personal Communication Service
UMTS	Universal Mobile Telecommunication Service
WLAN	Wireless Local Area Network

References

1. Quijano, J.L.A.; and Vecchi, G. (2012). Optimization of a compact frequency and environment-reconfigurable antenna. *IEEE Transactions on Antennas and Propagation*, 60(6), 2682-2689.
2. Aboufoul, T.; Alomainy, A.; and Parini, C. (2012). Reconfigured and notched tapered slot UWB antenna for cognitive radio applications. *International Journal of Antennas and Propagation*, 8 pages.
3. Ren, Z.; Li, W.; Xu, L.; and Shi, X. (2013). A compact frequency reconfigurable un-equal u-slot antenna with a wide tunability range. *Progress in Electromagnetics Research Letters*, 39, 9-16.
4. Qiu, Q.; Gong, S.-X.; Xu, Y.-X.; Cao, Y.; Duan, P.; and Chen, C. (2013). A novel pattern and frequency reconfigurable microstrip parasitic array. *Progress in Electromagnetics Research Letters*, 41, 149-158.
5. Cheng, C.X.; Zhang, F.-S.; and Yao, Y.-L. (2014). A compact microstrip patch antenna with reconfigurable feed network for polarization diversity. *Progress in Electromagnetics Research Letters*, 48, 67-73.
6. Li, K.; Li, L.; Zhu, C.; and Liang, C.-H. (2014). A new polarization reconfigurable microstrip antenna based on complementary split ring resonator. *Progress in Electromagnetics Research Letters*, 46, 119-125.
7. Rajeshkumar, K.V.; and Raghavan, S. (2015). A compact metamaterial inspired triple band antenna for reconfigurable WLAN/WiMAX applications. AEU - *International Journal of Electronics and Communications*, 69(1), 274-280.
8. Aghdam, S.A.; and Bagby, J.S. (2015). Resonator type for the creation of a potentially reconfigurable filtering band in a UWB antenna. *Progress in Electromagnetics Research Letters*, 52, 17-21.
9. Horestani, A.K.; Shaterian, Z.; Naqui, J.; Martin, F.; and Fumeaux, C. (2016). Reconfigurable and tunable s-shaped split ring resonators and application in band-notched UWB antennas. *IEEE Transactions on Antennas and Propagation*, 64(9), 3766-3776.
10. Qin, P.-Y.; Weily, A.R.; Guo, Y.J.; and Liang, C.H. (2010). Polarization reconfigurable U-slot patch antenna. *IEEE Transactions on Antennas and Propagation*, 58(10), 3383-3388.

11. Sun, C.; Zheng, H.; Zhang, L.; and Liu, Y. (2014). A compact frequency-reconfigurable patch antenna for beidou (COMPASS) navigation system. *IEEE Antennas and Wireless Propagation Letters*, 13, 967-970.
12. Li, T.; Zhai, H.; Wang, X.; Li, L.; and Liang, C. (2015). Frequency-reconfigurable bow-tie antenna for bluetooth, WiMAX, and WLAN applications. *IEEE Antennas and Wireless Propagation Letters*, 14, 171-174.
13. Panahi, A.; Bao, X.L.; Yang, K.; O'Conchubhair, O.; Ammann, M.J. (2015). A simple polarization reconfigurable printed monopole antenna. *IEEE Transactions on Antennas and Propagation*, 63(11), 5129-5134.
14. Yu, L.; Liu, P.; Meng, Z.; Wang, L.; and Li, Y. (2018). A planar printed nona-band loop-monopole reconfigurable antenna for mobile handsets. *IEEE Antennas and Wireless Propagation Letters*, 17(8), 1575-1579.
15. Madhav, B.T.P.; Rajiya, S.; Nadh, B.P.; and Kumar, M.S. (2018). Frequency reconfigurable monopole antenna with DGS for ISM band applications. *Journal of Electrical Engineering*, 69(4), 293-299
16. Su, S.-W. (2014). Compact four loop antenna system for concurrent, 2.4 and 5 GHz WLAN operation. *Microwave and Optical Technology Letters*, 56(1), 208-215.
17. Miller, P. (2014). The measurement of antenna group delay. *Proceedings of the 8th European Conference on Antennas and Propagation (EuCAP). The Hague, Netherlands.* 1488-1492.